20

CREEP IN CERAMICS

20.1 INTRODUCTION

Creep can most simply be described as the phenomenon of continuing plastic deformation under constant stress. Creep effects may be studied with other loading schedules, but the same basic processes are involved. Typically, creep in ceramics takes place at high temperatures under modest stress levels and with low strain rates. Creep is sometimes discussed as if it were a different phenomenon than plastic deformation and the latter is treated as if it occurred instantaneously when stress is applied.

Fundamentally, however, plastic deformation is not qualitatively different from creep. In this chapter the phenomenological description of creep in terms of stages is first given and then several important mechanisms of creep in ceramics are discussed. An excellent general reference on creep is Poirier (1985).

Creep in ceramics has been reviewed thoroughly by Cannon and Langdon (1983, 1988). These authors classify creep in ceramics into two categories

Mechanical Properties of Ceramics, Second Edition
By John B. Wachtman, W. Roger Cannon, and M. John Matthewson

depending on the way in which the creep rate depends on the stress. In the first category the creep rate depends on the stress to a power close to 1. In the second category the creep rate depends on stress to a higher power, typically approximately 3 or 5. Creep with a stress exponent of 5 is believed to take place as in metals by a dislocation motion with five independent slip systems operating. Diffusion plays a role associated with the freeing of tangled or pinned dislocations rather than with the primary transport process. Creep with a stress exponent of about 3 is taken to result from dislocation climb under conditions such that five independent slip systems cannot interpenetrate or when there are fewer than five independent slip systems operating.

Creep is most often measured under a constant stress. Figure 20.1 shows a typical creep curve. The creep strain ε resulting from application of constant stress is often written as

$$\varepsilon = \varepsilon_0 + \beta t^{1/3} + kt \tag{20.1}$$

Here ε_0 is the elastic strain and β and k are constants for a given material with a given microstructure (including defect structure) at a particular temperature. The second and third terms describe what is called, respectively, primary and steady-state creep. The justification for this equation is empirical; it fits much of the experimental creep data. If a dislocation mechanism controls creep, primary creep results from hardening as dislocations tangle with each other and eventually develop a steady-state substructure. If the Nabarro–Herring mechanism, described below, controls creep, the primary stage may be caused by grain growth. If creep is continued long enough, a tertiary stage is encountered, especially in metals. In tension this tertiary stage is an accelerating creep rate leading to failure.

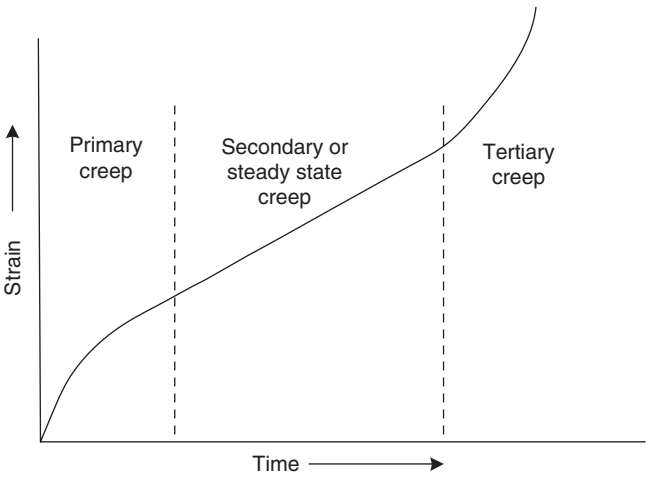

FIGURE 20.1 Typical creep curve measured under constant stress.

Most of the attention in creep studies is focused on steady-state creep or at least what is taken as steady-state creep. The assumption is made here that a sufficient period of time giving nearly constant creep rate is studied experimentally to justify the fitting of models for steady-state creep and these models are presented.

20.2 NABARRO–HERRING CREEP

Nabarro (1948) considered a small cube of material under a pure shear stress resulting from tension in one direction (say, the z direction) and sufficient compression in the x and y directions to give zero pressure. He showed that vacancies would flow from the face under tension to the faces under compression, causing a shear of the material so as to elongate it in the z direction and cause it to shrink in the x and y directions. The equilibrium atomic fraction of vacancies at temperature T is given by

$$N_v = \exp\left(-\frac{\Delta G_f}{kT}\right) \tag{20.2}$$

where ΔG_f is the Gibbs free energy of formation of one vacancy and k is Boltzmann's constant. The equilibrium concentration is then

$$C_0 = \frac{N_v}{\Omega} \tag{20.3}$$

where Ω is the atomic volume. Creation of a vacancy at the face under tension σ is assisted by a contribution $\sigma\Omega$ to the free energy, while extra free energy of the same amount is needed to create a vacancy at the face under compression.

The local equilibrium concentrations at the tension and compression faces, respectively, are then

$$C^+ = C_0 \exp\left(\frac{\sigma\Omega}{kT}\right) \tag{20.4}$$

$$C^- = C_0 \exp\left(\frac{-\sigma\Omega}{kT}\right) \tag{20.5}$$

There will be a flux of vacancies from the higher concentration face to the lower concentration face given by Fick's equation for diffusion,

$$J = -D_v \nabla C \approx \alpha D_v \frac{C^+ - C^-}{d} \tag{20.6}$$

where α is a numerical constant and d is the edge of the cube. The number of vacancies passing through an area d^2 per second, φ, is

$$\varphi = Jd^2 \tag{20.7}$$

The volume arriving per second is $\varphi\Omega$. Dividing by the area of a face, d^2, gives the elongation per second, and dividing this in turn by the length d gives the strain rate $\dot{\varepsilon}$:

$$\frac{d\varepsilon}{dt} \equiv \dot{\varepsilon} = \varphi \frac{\Omega}{d^3} \tag{20.8}$$

$$\dot{\varepsilon} = \frac{\Omega}{d^3} J d^2 = \frac{\Omega}{d} \alpha D_v \frac{C^+ - C^-}{d} = \frac{\alpha \Omega D_v C_0}{d^2} \left(\exp \frac{\sigma \Omega}{kT} - \exp \frac{\sigma \Omega}{kT} \right) \tag{20.9}$$

For $\sigma\Omega/kT < 1$

$$\dot{\varepsilon} = 2\alpha \frac{D_v \Omega^2 \sigma C_0}{kTd^2} \tag{20.10}$$

Recognizing that the self-diffusion constant D_l is given by

$$D_l = D_v \Omega C_0 \tag{20.11}$$

leads to

$$\dot{\varepsilon} = 2\alpha \frac{D_l \Omega \sigma}{d^2 kT} \tag{20.12}$$

Herring (1950) gave a thermodynamic treatment and considered the case of grains in a solid and found $\alpha = 16$ when there is no grain boundary sliding or $\alpha = 40$ when there is sufficient grain boundary sliding to completely relax shear stresses on the boundary. The usual creep experiment is done in simple tension. When Herring's result and the relationship of simple tensile stress to the stress system used above to give simple shear are taken into account, the result for complete grain boundary sliding is (Poirier, 1985; Cannon and Langdon, 1988)

$$\dot{\varepsilon} = 13.3 \frac{D_l \Omega \sigma}{d^2 kT} \tag{20.13}$$

where σ is now the tensile stress in a simple tensile test. The important characteristics of Eq. (20.13) is that $\dot{\varepsilon}$ is directly proportional to the stress and inversely proportional to grain diameter squared.

20.3 COMBINED DIFFUSIONAL CREEP MECHANISMS

The above derivation of Nabarro–Herring creep assumed only one diffusion path (through the solid grains) and only one diffusing species. In ceramics there are often two possible diffusion paths (through the grains or in the grain boundaries), as illustrated in Figure 20.2, and two diffusing species

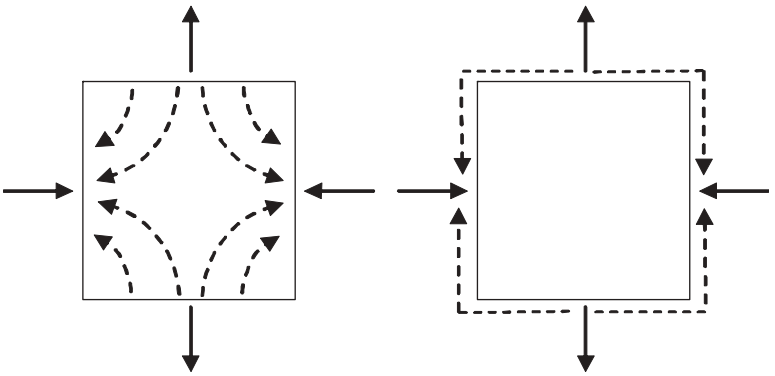

FIGURE 20.2 (a) Nabarro–Herring creep by lattice diffusion. (b) Coble creep by grain boundary diffusion.

(e.g., oxygen and aluminum in aluminum oxide). Cannon and Langdon (1988) have summarized the equations for these situations as presented in the following.

First we will write the Nabarro–Herring equation in a different format, which allows comparing diffusional creep equations with dislocation creep equations. Taking the atomic volume Ω as $0.7b^3$, where b is the magnitude of the Burgers vector, Eq. (20.13) may be written as

$$\dot{\varepsilon} = 9.3\frac{D_l \mu b}{kT}\left(\frac{b}{d}\right)^2\left(\frac{\sigma}{\mu}\right) \tag{20.14}$$

where μ is the shear modulus and d is the grain diameter. Equation (20.14) is written in such a way that terms in parentheses are dimensionless.

If the transport of matter is through the grain boundaries, the process is termed Coble creep (Coble, 1963). The diffusional creep equation then is

$$\dot{\varepsilon} = \frac{150\Omega\delta D_{gb}\sigma}{\pi d^3 kT} \tag{20.15}$$

where D_{gb} is the diffusion constant for transport in the grain boundaries and δ is the grain boundary width. Again writing Eq. (20.15) in universal format with $\Omega = 0.7b^3$, the creep rate is

$$\dot{\varepsilon} = 33.4\frac{D_{gb}\mu b}{kT}\left(\frac{\delta}{b}\right)\left(\frac{b}{d}\right)^3\left(\frac{\sigma}{\mu}\right) \tag{20.16}$$

Because the activation energy for grain boundary diffusion is less than that for diffusion through the grains, Coble creep is favored over Nabarro–Herring creep at lower temperatures. Because of the inverse cubic dependence on grain

size, Coble creep is favored over Nabarro–Herring creep at very small grain sizes.

Actually, Nabarro–Herring creep and Coble creep take place in parallel so that the total diffusional creep rate is given by

$$\dot{\varepsilon} = 9.3\frac{D_l \mu b}{kT}\left(\frac{b}{d}\right)^2\left(\frac{\sigma}{\mu}\right)\left[1 + 3.6\frac{D_{gb}}{D_l}\left(\frac{\delta}{d}\right)\right] \tag{20.17}$$

In a ceramic M_aX_β both anions and cations can diffuse, leading to (Gordon, 1973, 1975)

$$\dot{\varepsilon} = 9.3\frac{D_{a,\text{eff}} \cdot D_{c,\text{eff}}}{\alpha D_{c,\text{eff}} + \beta D_{a,\text{eff}}}\frac{\mu b}{kT}\left(\frac{b}{d}\right)^2\frac{\sigma}{\mu} \tag{20.18}$$

where

$$D_{i,\text{eff}} = D_{i,l} + 3.6D_{i,gb}\left(\frac{\delta_i}{d}\right) \tag{20.19}$$

and where i is a or c for the anion and cation, respectively.

Evans and Langdon (1976) considered the possibilities for the usual cases in which there are large differences in the diffusion rates. Their general conclusion is that the creep rate is controlled by the slower diffusing species along the faster diffusion path.

Li et al. (1999) presented evidence that grain boundary diffusion strongly affects the creep rate of polycrystalline Al_2O_3. When Al_2O_3 was doped with as little as 100 ppm rare earth additives (Y^{3+}, Nb^{3+}, La^{3+}), creep rates fell by two orders of magnitude. Even lower creep rates were achieved by codoping with Nb^{3+} and Zr^{4+}. Secondary ion mass spectrometry revealed that the dopants segregated to the grain boundaries. Wang et al. (2000) suggest the much larger rare earth ions substituted for the very small Al^{3+} ions in the grain boundary and relieved the stress in normally stretched bonds. Less free volume was now available for grain boundary diffusion. Since the dopants were expected to have affected only grain boundary diffusion, two possibilities exist: (1) $D_{Al,gb}$ or $D_{O,gb}$ were rate controlling and the rare earth additive decreased their grain boundary diffusion rate or (2) lattice diffusion controlled by one ion changed to the other ion. Originally, for instance, $D_{Al,l}$ controlled the creep rate because O^{2-} ions traveled rapidly through the grain boundary, that is, $(\delta/d)D_{O,gb}$ was higher than $D_{O,l}$ while $(\delta/d)D_{Al,gb}$ was lower than $D_{Al,l}$. With the addition of rare earth ions $D_{O,gb}$ decreased sufficiently so that O^{2-} ions must travel through the bulk and $D_{O,l}$ now controlled the creep rate.

20.4 POWER LAW CREEP

In this section the concept of creep by dislocation slip with the rate-controlling process being the thermally activated freeing of dislocations is summarized.

The succession of ideas is that of long- and short-range stress, thermal activation of dislocations over barriers, the balancing of hardening and recovery and the resulting Bailey–Orowan equation, and the Weertman model of creep by slip with rate control by climb.

Metals often creep with a steady-state creep rate varying with approximately the fifth power of the stress. Weertman (1957) developed a theory for glide of piled-up dislocations from an operating source with climb being the rate-controlling process. He obtained

$$\dot{\varepsilon} = \frac{B_2 \Omega D_l \sigma^{4.5}}{\mu^{3.5} M^{0.5} b^{3.5} kT} \tag{20.20}$$

where B_2 is a constant and M is the concentration of the active dislocation sources. Taking $B_2 = 0.2$ (Hazzledine, 1967; Cannon and Langdon, 1988) gives

$$\dot{\varepsilon} = \frac{0.14}{b^{1.5} M^{.5}} \left(\frac{D_l \mu b}{kt}\right) \left(\frac{\sigma}{\mu}\right)^{4.5} \tag{20.21}$$

Some ceramics exhibit stress dependence with a power near 5 and are assumed to creep by a dislocation mechanism of the Weertman type.

Metals or ceramics undergoing power law creep form a substructure within grains with the subgrains bounded by small-angle grain boundaries with an average size λ. The dislocation density within the grains is ρ. Cannon and Langdon (1988) conclude that ceramics deforming by dislocation creep show the same behavior as metals in that the average subgrain size is inversely related to the stress,

$$\frac{\lambda}{b} = \text{const} \times \frac{\mu}{\sigma} \tag{20.22}$$

The constant is in the range of 20–30 for ceramics and is typically 20 for metals. The normalized dislocation density within subgrains for ceramics was found to be given by

$$b\rho^{1/2} = \text{const} \times \frac{\sigma}{\mu} \tag{20.23}$$

Here the constant ranges from 1 to 2 for ceramics and is around 1 for metals.

Other ceramics exhibit a stress dependence with a power near 3. Cannon and Langdon (1988) examined theories giving this type of stress dependence and concluded that the most likely was a mechanism of creep through climb of dislocations from Bardeen–Herring sources. The theory predicts

$$\dot{\varepsilon} = 0.22 \frac{D_l \mu b}{kt} \left(\frac{\sigma}{\mu}\right)^3 \tag{20.24}$$

Chokshi and Langdon (1991) examined the power law creep of ceramics and concluded that there are two broad categories of behavior: A stress exponent

close to 5 represents control by dislocation climb and fully ductile behavior whereas a stress exponent close to 3 arises from control by climb from Bardeen–Herring sources under conditions where there are less than five interpenetrating independent slip systems.

20.5 COMBINED DIFFUSIONAL AND POWER LAW CREEP

Cannon and Langdon (1988) compared the creep rates of ceramics with the creep rates of metals using the universal form of the creep equation. Equations (20.14), (20.16), (20.20), and (20.23) may all be written in the form

$$\dot{\varepsilon} = B\frac{D\mu b}{kT}\left(\frac{b}{d}\right)^{p}\left(\frac{\sigma}{\mu}\right)^{n} \tag{20.25}$$

where $p = 0$ for dislocation mechanisms, $p = 2$ for Nabarro–Herring creep, and $p = 3$ for Coble creep. The parameter D does not specify whether it is a lattice or a grain boundary diffusion coefficient and B incorporates other constants and grain boundary widths. Rearranging yields

$$\frac{\dot{\varepsilon}kT}{D\mu b} = B\left(\frac{b}{d}\right)^{p}\left(\frac{\sigma}{\mu}\right)^{n} \tag{20.26}$$

Thus a universal curve for dislocation mechanisms plots $\dot{\varepsilon}kT/(D\mu b)$ versus (σ/μ) on a log–log scale. Diffusional creep results may be included on the same plot as long as the grain size is specified. Such a plot is shown in Figure 20.3. A summary of the creep data of ceramics is reviewed in Cannon and Langdon (1988), and it is shown that most results where $n \simeq 1$ fit the Nabarro–Herring equation provided D_{cation} is used as the diffusion coefficient. On the other hand for power law creep D_{anion} is used. Under these assumptions and noting that in most cases $D_{\text{cation}}/D_{\text{anion}} = 100$, Figure 20.3 summarizes the creep data from the literature for both coarse-grained ceramics which exhibit power law creep and fine-grained ceramics which exhibit diffusional creep. Literature power law creep data in metals superimpose reasonably well on the ceramic power law creep data. Diffusional creep is not often observed in metallic systems. Because the diffusion coefficient is the most strongly varying factor, it is concluded that creep rates depend primarily on the diffusion rates independent of whether they are metals or ceramics. The large difference in the mobility of dislocations in metals and ceramics is not important since freeing of dislocations by dislocation climb controls the creep rate. It may further be observed in Figure 20.3 that the stress range over which diffusional creep occurs widens as the grain size is decreased. It is because the typical grain size for advanced ceramics is much smaller than in typical polycrystalline metals that diffusional creep is most often observed in ceramics.

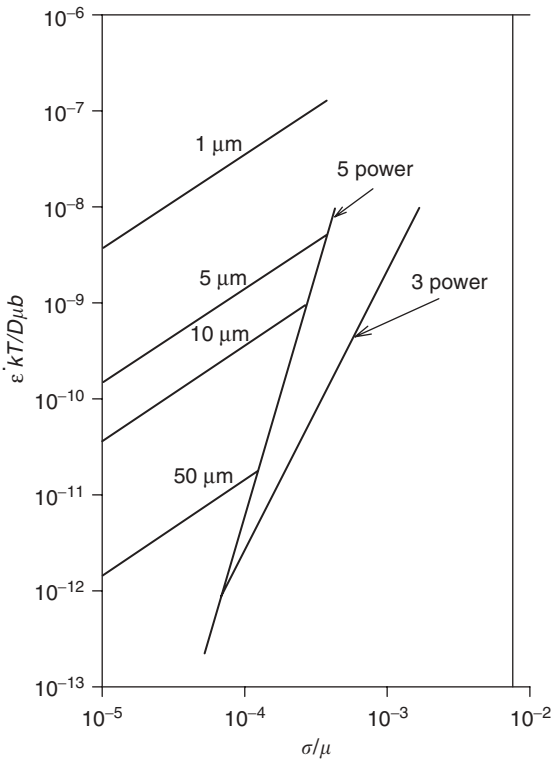

FIGURE 20.3 Universal curve for diffusional and dislocation creep mechanisms. It is assumed that $D_{\text{cation}}/D_{\text{anion}} = 100$ and that diffusional creep is controlled by the anion and dislocation creep by the cation. (From Cannon and Langdon, 1988. Reprinted with permission from Springer Verlag).

20.6 ROLE OF GRAIN BOUNDARIES IN HIGH-TEMPERATURE DEFORMATION AND FAILURE

Grain boundaries often play a crucial role in deformation and fracture of ceramics. We follow Langdon (1982, 1991a, b, 1993a, b, 1994a, b) in presenting a summary considering behavior of metals and ceramics. Grain boundaries play two important but conflicting roles in deformation: contributing to the deformation and promoting local cracking and ultimate failure. The grain size determines the degree of grain boundary contribution to deformation and failure. Langdon defines four grain sizes in this regard—macroscopic, mesoscopic, microscopic, and nanoscopic:

- Macroscopic grains are large enough, typically with grain diameter $d > 1000\,\mu\text{m}$, so that grain boundaries play no significant role in deformation.

- Mesoscopic grains are smaller but still large enough that the grain boundaries make a relatively minor contribution to deformation (such as in grain boundary sliding as a secondary process) but the boundaries may be dominant in controlling fracture. In metals typical mesoscopic grains range from 10 to 1000 μm in diameter. For materials deforming by dislocation slip, a substructure forms within mesoscopic grains consisting of subgrains of average diameter λ with small misorientations between adjacent subgrains.
- Microscopic grains are still smaller (typically 10–0.01 μm) and grain boundaries play a dominant role in flow and often also in fracture.
- Nanoscopic grains are still smaller and are only beginning to be investigated as processing methods for making polycrystalline materials with grains in this range are still being developed. It is anticipated that grain boundaries will contribute most of the deformation in these materials.

Grain boundaries are important for ultimate failure in tension because they provide sites at which cavities can be nucleated and paths for the growth of cavities into intergranular cracks. For ceramics these processes are significant in damage-assisted creep and subsequent failure. However, under suitable conditions, both metals and ceramics with microscopic grain size can undergo large tensile deformations before failure, as discussed in a later section on superplasticity.

20.7 DAMAGE-ENHANCED CREEP

An additional feature of creep in ceramics that has not been considered so far is damage-enhanced creep. It is often observed, especially at higher stresses in ceramics with a viscous phase in the grain boundaries, that voids form at the grain boundaries as creep continues. Results of Wiederhorn et al. (1988) on siliconized silicon carbide are reviewed here to illustrate the phenomenon. Damage-enhanced creep has also been reported by other investigators in various materials, including lithium zinc silicate glass ceramics (Morrell and Ashbee, 1973), reaction-bounded silicon nitride (Birch et al., 1978), siliconized silicon carbide (Carroll and Tressler, 1988), and SiAlON–YAG ceramics (Chen et al., 1991).

The experiments of Wiederhorn et al. (1988) were done with a siliconized silicon carbide, KX01, made by SOHIO Corp. This material is approximately 33% silicon by volume and contains grains of silicon carbide ranging from 2 to 5 μm in diameter. These authors measured creep at 1300°C in tension and compression and found that the creep rate in tension was 30 times or greater than the creep rate in compression at the same stress. Furthermore, the dependence of creep rate on stress was bimodal in both cases. Their results are summarized in Figure 20.4, a log–log plot of creep rate as a function of

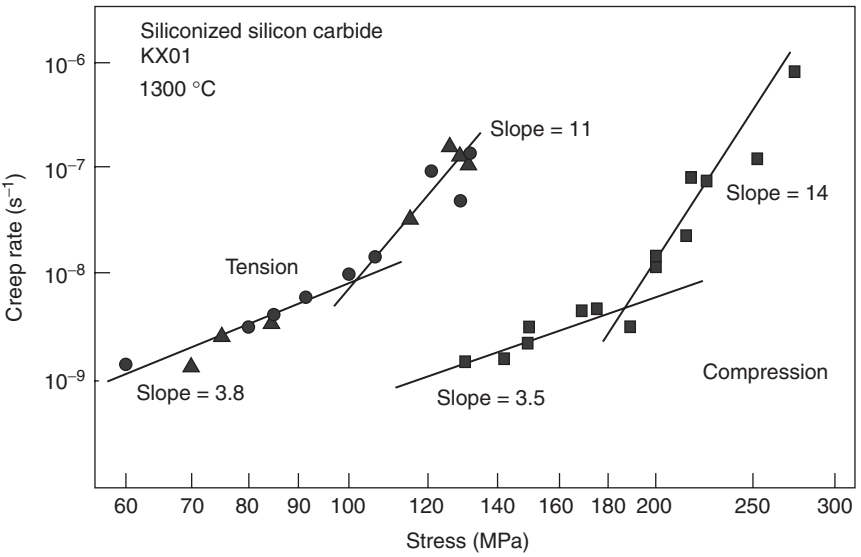

FIGURE 20.4 Stress dependence of creep rate. (From Wiederhorn et al., 1988. Reprinted by permission of the American Ceramic Society.)

stress. The results can be described by a power law equation of the form

$$\dot{\varepsilon} = k\sigma^n \tag{20.27}$$

where k and n are constants. For creep in tension $n = 3.5$ at stresses below 100 MPa and $n = 11$ for higher stresses. For creep in compression $n = 3.5$ for stress below 200 MPa and $n = 14$ for higher stresses. The authors attribute the creep in the range of stresses corresponding to the lower n values to power law deformation in the silicon phase. They find some formation of voids (cavitation) at tensile stresses as low as 75 MPa, but very much more cavitation in experiments at 100 MPa for 100 h. They attribute the higher creep rates above 100 MPa in tension to the effects of cavitation. For creep in compression in the stress range corresponding to the lower n values, power law creep is also assumed. The authors suggest that friction between silicon carbide grains affects the stress on the silicon phase and hence the creep rate. It is plausible that these frictional forces would be greater in compressive creep and so increase the stress required to achieve the same creep rate. The authors searched for cavitation in the compressive creep specimens but did not find evidence of it. The cause for the change to $n = 14$ at higher stresses in compression was not determined.

A study showing the combined effect of a basic creep mechanism and damage-assisted creep in siliconized silicon carbide was reported by Carroll and Tressler (1989). They found a threshold for creep damage of 132 MPa at

1100°C. Below this stress the stress exponent was about 4. At stresses above the creep damage threshold the stress exponent increased with increasing stress to around 10 at 172 MPa. The activation energy for creep also increased with increasing stress above the threshold. Creep below the stress threshold was attributed to dislocation activity in the silicon phase. Above the stress threshold for damage, cavities formed and contributed to the creep strain. Models developed by Raj (1982) and Hasselman and Venkateswaran (1984) were used to separate the damage component, leading to the conclusion that the remaining component of the creep strain is still well described by a stress exponent of 4 to the highest stresses used.

20.8 SUPERPLASTICITY

Many polycrystalline materials, including some ceramics, can sustain very large creep deformations (several hundred percent) in uniaxial tension at high temperature (typically above one-half the absolute melting temperature) before failing (Nieh and Wadsworth, 1990b). Fine grain size (a few micrometers or less) and an equiaxed structure are required. A striking feature of superplastic behavior is that grain shape does not change appreciably during deformation, in contrast to normal plastic deformation in ductile polycrystalline materials. In the latter, the grains typically elongate to the same extent as the specimen as a whole.

Of the ceramic materials exhibiting superplastic deformation, Y–TZP (Y_2O_3–ZrO_2) is by far the most widely studied. It fills the necessary requirements of a fine grain size, typically 0.4-μm-diameter and equiaxed grains. According to Chen and Xue (1990), an additional feature of Y–TZP necessary for high elongations is a low grain boundary energy, which reduces the tendency toward cavity formation along the grain boundaries.

It is generally agreed that superplastic deformation takes place by grain boundary sliding, but at the time of writing there is still much discussion about exactly how this can occur. To illustrate superplastic deformation by grain boundary sliding, Figure 20.5 shows grains on a polished surface of a Y–TZP specimen strained in compression to 0, 14, 28, 42, and 56%. Usually superplastic deformation is defined by tensile deformation, but compression tests can still be used to study the mechanism. It is observed in Figure 20.5 that grains do not significantly change size or shape but they change position relative to one another. Grain 1 comes together with grains 6 and 7, grains 3 and 5 move apart, and grain 4 disappears into the surface. The specimen becomes shorter because grains switch positions, leading to a smaller number of grains along the length of the specimen rather than grains themselves changing shape. According to Duclos (2004), 80% of the deformation can be accounted for from these grain-switching events. If the specimen were deformed instead, in tension the number of grains along the length of the specimen would increase and new grains would appear on the surface.

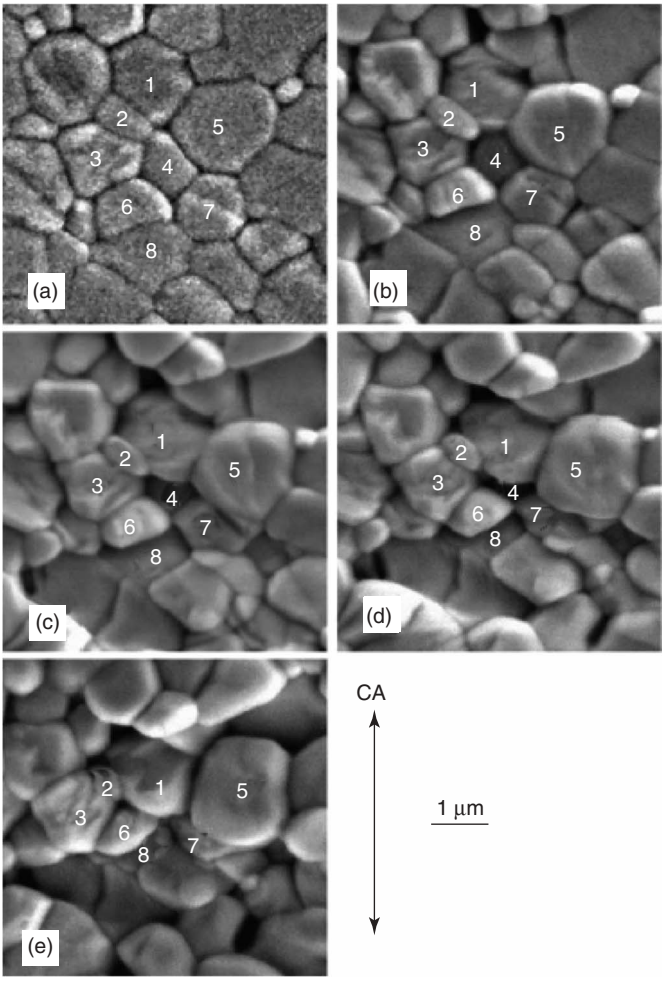

FIGURE 20.5 Polished surface of Y–TZP after (a) 0%, (b) 14%, (c) 28%, (d) 42%, and (e) 56% deformation in compression: CA = compression axis. Grain 4 disappears into the surface and grain 1 comes together with grains 6 and 7. (After Duclos, 2004. Reprinted with Permission of Elsevier Press.)

Grain-switching events may be local or may extend across the specimen. If shear occurs in straight lines across the entire specimen, it is called cooperative grain boundary sliding. Figure 20.6 depicts cooperative grain boundary sliding in a schematic depiction using circular grains. Each row of grains along the dark lines shifts one grain distance in the direction of the arrows. The picture illustrates how under compressive strain grain 2 can disappear from the surface while grains 1 and 3 above and below grain 2 come together. One

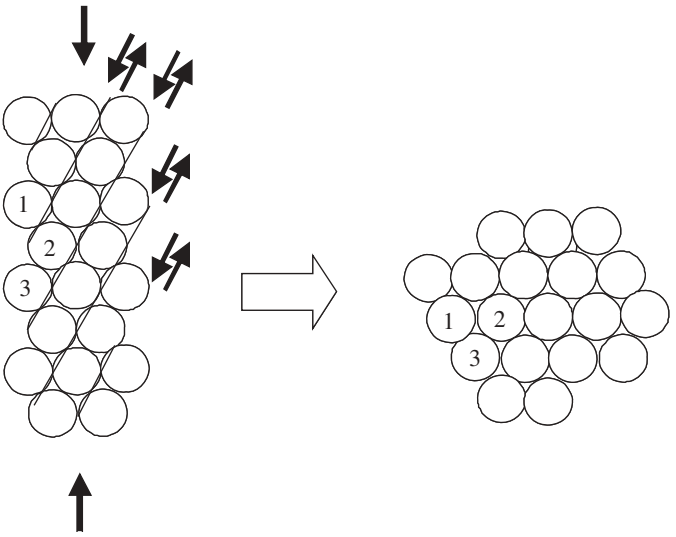

FIGURE 20.6 Grains represented as circles illustrate cooperative grain boundary sliding. Grain slide one grain length downward to left. Grain 2 disappears from the surface and grains 1 and 3 come together.

can visualize tensile strain by going from the figure on the right to one on the left rather than from the left one to the right one. Then grain 2 appears on the surface.

It is somewhat more difficult to depict a local grain-switching event. Nevertheless the literature contains many attempts at modeling these local switching events that are reviewed by Zelin and Mukherjee (1996). Most of these models, however, require temporary creation of voids or intermediate steps of greatly altered grain shape. There is some evidence from micrographs such as Figure 20.5 that bands of grain boundaries shear across the entire specimen, but this was not seen by Duclos (2004). Thus it is uncertain whether cooperative grain boundary sliding can account for most of the strain. Regardless of the manner in which grain-switching events occur, grain boundary sliding cannot take place without some sort of accommodation at grain boundary triple points because grain boundary are not aligned along a flat plane. Some possibilities that have been suggested are diffusional accommodation, dislocation accommodation, and grain boundary migration to straighten out the plane of the grain boundary. Ashby and Verrall (1973) proposed grain-switching events which require a combination of diffusional creep and grain boundary migration. There is certainly abundant evidence that superplastic deformation enhances grain boundary migration and so grain boundary migration could easily play an important role in superplastic deformation.

One accommodation mechanism which has been popular in explaining how grains move past each other is Gifkin's 1976 core-and-mantle mechanism,

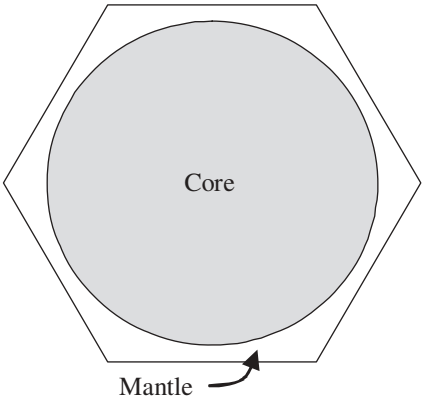

FIGURE 20.7 Core-and-mantle model.

illustrated in Figure 20.7. The core is rigid and the mantle is fluid, deforming by grain-boundary-enhanced processes such as grain boundary diffusion and solution precipitation. One can imagine how grains might slide past each other if the corner and edges are fluid.

The question of what mechanism controls the creep rate will again be illustrated by the results for Y–TZP. Superplasticity in Y–TZP, as with superplastic metals, shows several regions of different stress dependence on creep rate in which Eq. (20.27) holds. In region II, $n = 2$ in both ceramics and metals. In region I at low stresses (low strain rates), $n > 2$. [Region I is not observed in Y–SZP containing >0.1 wt. % total impurity content, according to Jimenez-Melendo et al. (1998).] There is good evidence that in high-purity Y–TZP there exists a threshold stress below which the grain boundary sliding mechanism no longer operates and creep is very slow. In the transition between the threshold stress and the stress of region II the stress exponent n is high. Jimenez-Melendo et al. (1998) reviewed the large amount of literature on Y–TZP creep and concluded that the creep rate behavior in region II is controlled by Zr^{4+} ion diffusion through the lattice and that $\dot{\varepsilon}/D_{Zr^{4+}}$ agrees very well for a given σ/E with $\dot{\varepsilon}/D_\ell$ for superplastic metals whose creep rate is controlled by lattice diffusion. In accordance with Nabarro–Herring creep, the creep rate is proportional to $1/d^2$.

Superplasticity in ceramics has been considered as a forming mechanism. A potential problem is the development of internal voids. Ma and Langdon (1993) have studied superplastic deformation at 1723 K of dense TZP (3 mol % yttria) with a grain size of 0.5 μm. For strain rates of 0.0028, 0.00028, and $0.000028\,s^{-1}$, the engineering strains at failure were 85, 195, and 355%, respectively. Cavitation took place in each case, but the amount at failure increased with increasing strain rate. They concluded that cavitation is likely to be a problem in materials with very small grain sizes because of the large number of grain boundaries providing fast diffusion paths to feed cavity

growth. In superplastic metallic alloys the superplastic strain is limited by necking. It can be shown that the stress exponent n in Eq. (20.27) determines the sensitivity to necking of a particular material.

Assuming constant volume for plastic deformation and substituting in Eq. (20.27) yield

$$\dot{\varepsilon} = \frac{1}{L}\frac{dL}{dt} = -\frac{1}{A}\frac{dA}{dt} = k\sigma^n \tag{20.28}$$

so, since $\sigma = F/A$,

$$\frac{dA}{dt} = -kF^n A^{(1-n)} \tag{20.29}$$

One can now consider what would happen under constant-force creep conditions to a portion of the specimen in which the cross-sectional area A_2 is slightly smaller than the rest of the specimen, A_1, so that $A_2/A_1 < 1$. If $n = 1$ and, therefore, $1-n = 0$, the rate of decrease of the cross-sectional area is constant everywhere. If $n > 1$ so that $1-n = -\delta$ with δ positive, then

$$\frac{d(A_2/A_1)}{dt} = \left(\frac{A_1}{A_2}\right)^{\delta} \tag{20.30}$$

The right-hand side of Eq. (20.30) is a positive number greater than 1 so that the smaller cross-sectional area decreases faster than the larger cross-sectional area. Thus as n approaches 1 the tendency to necking decreases. Langdon (1982) has shown that the total creep strain before failure correlates well with n for many metals and metal alloys. The lower n values and highest total strain in metals and metal alloys is in region II where $n \cong 2$.

Chen and Xue (1990) have shown that percent elongation to failure of superplastic ceramics does not correlate well with n but does correlate well with the applied tensile stress. That is, elongation to failure is approximately inversely related to the tensile stress. It is not unexpected that elongation to failure is inversely related to stress and not to n, which is a necking sensitivity parameter since necking in ceramics is not generally observed and would not be expected because n usually approximates 1. On the other hand, failure of ceramics is very sensitive to formation of cavities along grain boundaries, as discussed in Chapter 21, and cavity formation is very sensitive to tensile stress. Thus, to achieve a high tensile strain, a ceramic must have very low creep resistance so that a large amount of strain can be achieved at a low stress and it must be very resistant to cavitation along grain boundaries. The most outstanding result at the time of writing is the result of Kim et al. (2001), who reported superplastic tensile deformation of 1050% in 26 s in a triphasic Al_2O_3–$MgAl_2O_4$–ZrO_2 ceramic at 1650°C. The average grain size was 0.21 μm.

Other unique features of superplastic ceramics as compared to superplastic metals and alloys from Langdon (1991b) are as follows. In superplastic metals

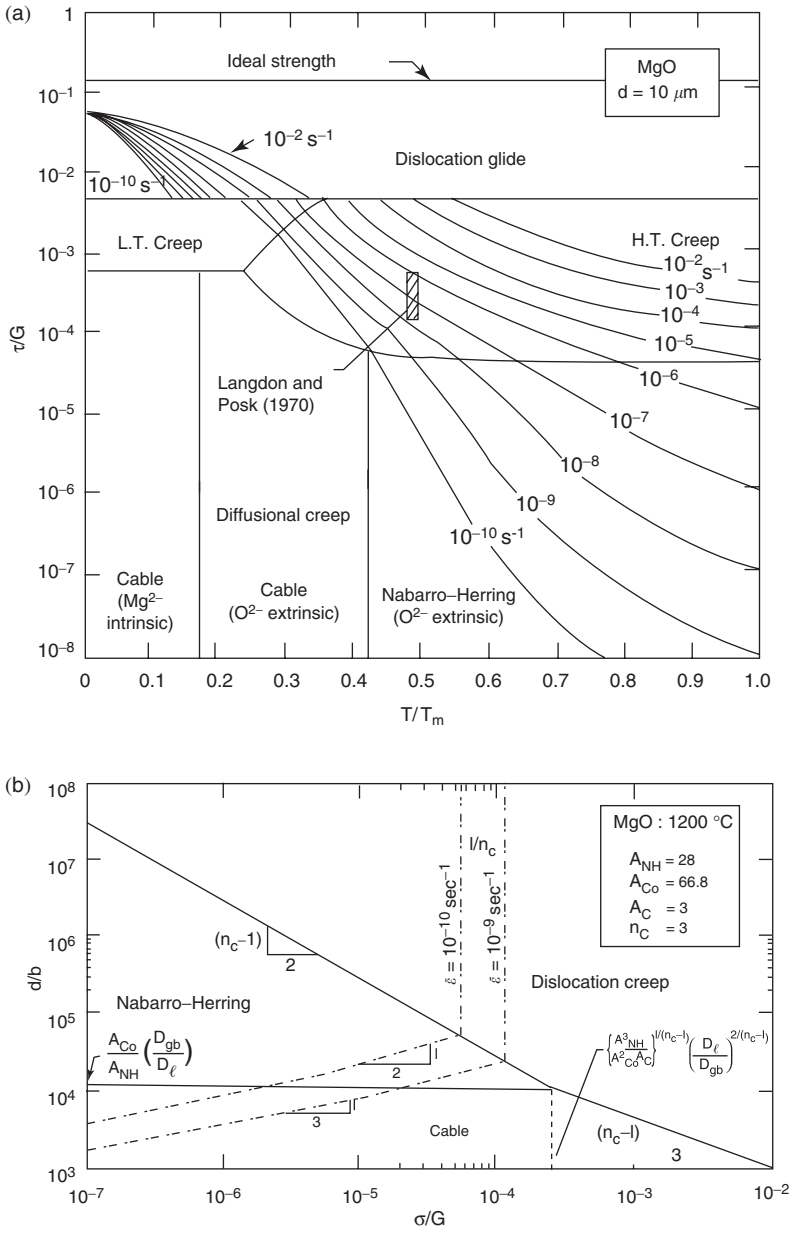

FIGURE 20.8 Deformation mechanism maps for MgO with (a) 10-μm grain size, and (b) at 1200°C. (Langdon and Mohamed, 1976. Reprinted with permission of Springer Verlag.)

and metallic alloys grain size does not affect the value of n, whereas in superplastic ceramics n increases as d decreases. Maximum cavitation occurs at the slowest strain rates in superplastic metals and metallic alloys whereas maximum cavitation occurs at the fastest strain rate in superplastic ceramics.

20.9 DEFORMATION MECHANISM MAPS

A very useful way of summarizing the dominant deformation mechanisms in a single drawing was apparently first suggested by Weertman and Weertman (1983) and has been developed by Ashby and his collaborators (Ashby, 1972; Frost and Ashby, 1982). The basic concept of these authors was to show, for a given grain size, the regions of stress and temperature in which each deformation mechanism dominates. Langdon and Mohamed (1976) have also presented diagrams of this type but for a constant temperature where stress and grain size are the variables. The border between two regions is the line along which the neighboring mechanisms have equal strain rates. Several types of plots are possible, but the most useful is a plot of log normalized stress (stress divided by the shear modulus), homologous temperature (absolute temperature divided by the melting temperature), or log normalized grain size (grain diameter divided by the Burgers vector). Two such plots for MgO are shown in Figure 20.8(a) and (b). In Figure 20.8(a), for MgO of 10 μm grain size, Langdon and Mohamed (1976) indicate a region where the dominant diffusional flow mechanism is controlled by magnesium diffusion in the boundary, another at higher temperatures controlled by oxygen in the boundary, and still another at a still higher temperatures where oxygen diffusion in the lattice is controlling. In these plots *intrinsic* and *extrinsic* refer to creep controlled by intrinsic or extrinsic diffusion.

A second type of deformation map shown in Figure 20.8(b) is at constant temperature (Langdon and Mohamed, 1976, 1978; Langdon, 1980). The axes are homologous grain size (grain size divided by the magnitude of the Burgers vector) and homologous stress (stress divided by the shear modulus). This type of deformation map shows the regions in which the predominant deformation mechanism is Nabarro–Herring creep, Coble creep, or dislocation creep. Lines of constant strain rate are overlaid on both of these maps.

PROBLEMS

1. Under 100 MPa stress a certain polycrystalline alumina underwent 5% strain in 25 h at 1500°C. The steady-state strain rate was measured to be $5 \times 10^{-7}\,s^{-1}$. Estimate the strain after only 1 h? Assume $E_{Al_2O_3}(1500°C) = 380$ GPa. Also assume there was a primary creep stage.

2. The creep rate of polycrystalline alumina of grain diameter $d = 18.4\,\mu m$ exhibited a stress exponent $n = 1.2$, an activation energy $Q_c = Q_{diffusion} =$